

# Formulation and optimisation of the probability matching method for radar reflectivity and rain rate in the Darwin region

**Xudong Sun**

Cooperative Research Centre for Catchment Hydrology,  
Department of Civil Engineering, Monash University, Australia

**T. D. Keenan**

Bureau of Meteorology Research Centre, Australia

and

**R. G. Mein**

Cooperative Research Centre for Catchment Hydrology,  
Department of Civil Engineering, Monash University, Australia

(Manuscript received August 1998; revised February 1999)

The focus of this paper is the estimation of rainfall from radar and rain-gauge networks. This study has further developed the probability matching method by introducing formulae by which radar reflectivity and rain rate relationships can be parametrised by assuming they fit known probability distributions. It is shown that rain rate ( $R$ ) and radar reflectivity ( $Z$ ) are basically log-normally distributed; hence respective population means and standard deviations provide the required probability distributions. A probability matching technique is developed based on this assumption. In practice the use of truncated log-normal distributions is found to be necessary to give the best fit in the development of  $Z$ - $R$  relations. Results presented for the Darwin region indicate reasonable agreement between rainfall values obtained with this approach and those employing traditional power law relationships and empirically based probability matching methods.

The effects of threshold values are also evaluated using an error process analysis and an optimisation algorithm to minimise the nonlinear object function of rainfall estimation. The optimised thresholds for the truncated log-normal distributions of radar reflectivity and rainfall in Darwin, Australia, are found to be around 21 dBZ and  $1.2 \text{ mm h}^{-1}$  respectively.

## Introduction

Many applications in meteorology and hydrology require accurate quantitative rainfall estimation. Weather radar is a remote sensing tool that can esti-

mate rainfall over a large area, in real time with high spatial and temporal resolution. Compared to radar, current rain-gauge networks are often too sparse to measure rainfall with adequate spatial and temporal scales, especially for intense convective storms when significant rainfall occurs. In this case, a ground truth

*Corresponding author address:* Xudong Sun, Bureau of Meteorology Research Centre, GPO Box 1289K, Melbourne, Vic. 3001, Australia

rain-gauge network is often employed to adjust and calibrate radar rainfall measurements.

The basic principle of radar rainfall measurement relies on the quantitative measurement of energy scattered by rain drops. Rainfall estimation from radar reflectivity, however, is a complex problem requiring numerous quality control and processing steps. For hydrometeorological applications, the relation between radar observations and rain rates can be obtained by means of theoretical, empirical and/or statistical approaches. Radar reflectivity ( $Z$ ) and rain rate ( $R$ ) relations based on power laws and the probability matching methods are among the main algorithms used so far.

The traditional power law method for rainfall estimation from radar is basically of the following form:

$$Z = AR^\alpha \quad \dots 1$$

where  $Z$  is the radar reflectivity factor ( $\text{mm}^6/\text{m}^3$ ) and  $R$  is the rain rate ( $\text{mm h}^{-1}$ );  $A$  and  $\alpha$  are parameters.

This method is based on the theory that both  $Z$  and  $R$  are functionally related to the rain droplet distributions. The determination of the parameters  $A$  and  $\alpha$  in the  $Z$ - $R$  relationship has been the subject of many years of endeavour, with perhaps hundreds of  $Z$ - $R$  relationships published. However, as indicated by Battan (1973), significant differences in rain intensity (up to a factor of five) at equal reflectivity are evident in these relationships.

The probability matching method (PMM) was first used by Calheiros and Zawadzki (1987). This method assumes that, if two random variables such as  $R$  and  $Z$  are functionally related, a transformation of the following form can be invoked:

$$p(R_i)dR = p(Z_i)dZ \quad \dots 2$$

where the pairs of ( $R_i$ ,  $Z_i$ ) define the PMM  $Z$ - $R$  relationship, with  $i$  varying to encompass the probability range 0 to 100%.

Alternatively, we can write the cumulative distribution functions:

$$\int_0^{R_i} p(R)dR = \int_0^{Z_i} p(Z)dZ \quad \dots 3$$

For the unconditional probability distribution function (PDF), integration is from zero to  $R_i$ ; for a non-zero conditional PDF, the integration begins at a threshold.

The latter approach was further developed by Rosenfeld et al. (1995a, 1995b), with the  $Z$ - $R$  relationship determined by matching the probabilities of

$R$  and  $Z$  over small time and space windows. The initial results indicated PMM approaches produced better rainfall estimates than obtained by the traditional power law techniques, primarily because the technique made allowance for varying distributions of rainfall in time and space.

The previous PMM techniques are based on empirical look-up tables, i.e., one gets an observation of radar reflectivity dBZ, then employs the look-up table to obtain the corresponding rainfall. This produces a matched  $Z$  and  $R$  relationship, thus defining the PMM curve. However, the PMM reflects the statistical characteristics of the rainfall and radar fields. This implies that if the inherent distributions representing local climatological characteristics of  $R$  and  $Z$  are of a known form, basic statistical parameters may be capable of parametrising the PMM relationships. This could simplify the PMM developmental procedure. Also error processes inherent in PMM have not been addressed in previous work.

This study investigates characteristics of rainfall rate and radar reflectivity PDFs, the way these characteristics can be employed to parametrise PMM techniques, and considers some aspects of error analysis processes. The results provide a basis for the parametrisation of PMM techniques and some discussion relevant to optimisation processes important in the derivation of PMM rainfall estimation procedures; furthermore, they provide a simple  $Z$ - $R$  relationship derived for the Darwin area.

## Radar and rain-gauge data

The radar data for this study were obtained from a 5.3 cm wavelength Doppler weather radar located at Darwin, Australia. The basic characteristics of the Darwin, Bureau of Meteorology (BoM) radar are listed in Table 1. At this site, the raw radar data were recorded every 10 minutes; Polar Constant-Altitude Plan Position Indicator (CAPPI) radar reflectivity fields at 1.5 km height with 1 degree by 1 km resolution were used as the primary radar data source.

**Table 1. Characteristics of the Darwin Doppler radar.**

Antenna size	4.2 m
Beamwidth	0.9°
Gain	45 dB
Polarisation	Horizontal
Wavelength	5.33 cm
Peak power	250 kW
PRF	Variable
Pulse width	1 $\mu$ s
Data recording	Lassen
Location	12.27°S, 130.56°E

The rain-gauge data were from a network of 25 tipping-bucket rain-gauges located within 150 km of the radar. Data from these gauges had a temporal resolution of 1 min.

The wet season rainfall is usually characterised by mesoscale tropical precipitation patterns in Darwin, with a wet season beginning in late December and extending to April of the next year. As discussed by Keenan et al. (1988) and Keenan and Carbone (1992), there are two periods in the season; one is a Monsoon-type and the other a Break-type period with rainfall almost every day. For this study, 79 rainfall days occurring during the 1993-94 season were studied; a period which included several major rainfall events. For example, the 27 February to 2 March 1994 period represents a monsoon system with extensive convective and stratiform precipitation.

## Probability matching of rainfall and reflectivity

### Quality control

Basic quality checks were performed to ensure that the rainfall and radar data were consistent, statistically significant, and not representing biased probability distributions. First, for every gauge station, time series of radar (10-minute interval) and rain-gauge data were plotted along with their basic statistical parameters (mean, standard deviation and correlation coefficients). Then histograms of rainfall rate and reflectivity were plotted, and associated PDFs calculated. The radar and rainfall PDFs were then matched using the approach of Atlas et al. (1990), and Rosenfeld et al. (1993), i.e. equivalent percentiles of the probabilities of  $R$  and  $Z$  are calculated using an interpolation technique.

Generally, the above showed:

- the data were of good quality with radar and gauge data showing similar statistical characteristics for each gauge location;
- the PMM curves calculated from Eqn 3 showed clearly a range-dependence as found by others, e.g., Calheiros and Zawadzki (1987), Rosenfeld et al. (1993). This is mainly because the radar beam-filling changes with distance;
- the rainfall data were stationary, and the expectation of rainfall accumulation was constant over the whole field;
- the rainfall and reflectivity data were approximately distributed log-normally. This important characteristic will be discussed in a later section.

### Conditional probability matching

Conditional probability matching means that some threshold is applied when matching radar and reflectivity data.

Retrieved PMM  $Z$ - $R$  relationships are very sensitive to the imposition of any radar and rain-gauge rainfall thresholds ( $Z_0$ ;  $R_0$ ). It can be seen in Figs 1 and 2 that the results of applying PMM procedures with the Darwin radar and rainfall data are quite different when two different thresholds are chosen ( $R_0 > 0$ ,  $Z_0 = 3$  dBZ and  $R_0 = 1.2$  mm h<sup>-1</sup>,  $Z_0 = 21$  dBZ). Because many low  $R$  samples occur near the lower thresholds, once the thresholds are changed a significant proportion of rainfall samples become truncated. This, in turn, affects the matching of the probability distribution functions. Therefore, different  $R_0$  and  $Z_0$  values influence the resultant PMM relationship. For example, comparison of Figs 1 and 2 shows use of the threshold values  $R_0 > 0$ ,  $Z_0 = 3$  dBZ results in more rainfall in low reflectivity regimes than that with the higher thresholds. A detailed discussion of this effect will follow in Sections 4 and 5. For the purposes of inter-comparison, Figs 1 and 2 also show two power law  $Z$ - $R$  relationships ( $Z = 70R^{1.25}$ ; Steiner et al. (1994) and  $Z = 200R^{1.6}$ ; Battan (1973)). Rainfall retrieved by the PMM employing the higher thresholds (Fig. 2) seems generally more consistent with the estimates obtained by the power law.

The matching of gauge rainfall and radar reflectivity PDFs is valid only if statistically consistent datasets are employed. Variations in the statistical characteristics of the two datasets can arise for many reasons including the following:

- rain-gauge measurements have their own minimal discernible rain intensity threshold and are influenced by environmental factors, primarily wind speed, and others;

**Fig. 1** Probability matching results of rainfall and radar reflectivity with thresholds of  $Z_0 = 3$  dBZ;  $R_0 > 0$  mm/h.

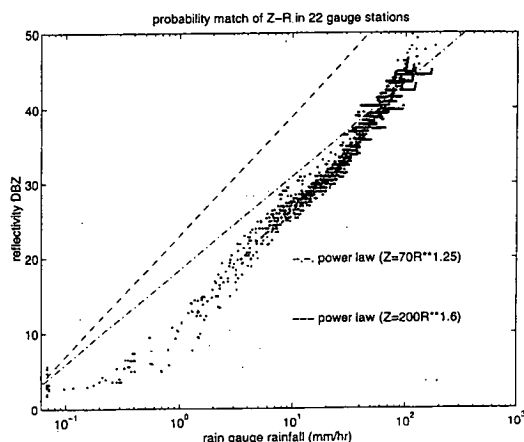
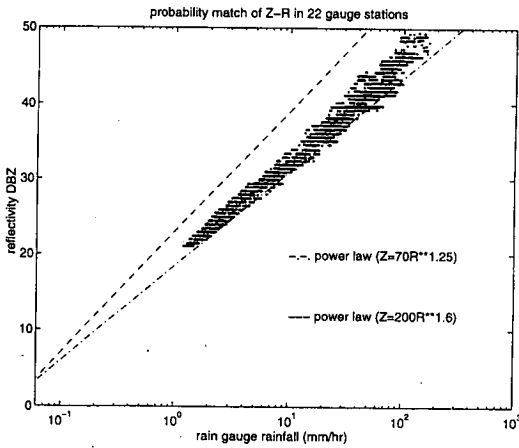


**Fig. 2** Probability matching results of rainfall and radar reflectivity with thresholds of  $Z_0=21$  dBZ;  $R_0=1.2$  mm/h.



- (b) the gauge and radar have different sampling volumes;
- (c) radar noise levels mean there is a range dependent threshold for radar rainfall detection;
- (d) radar ground echoes or clutter can possibly be interpreted as precipitation echoes and beam blockage can affect radar returns;
- (e) radar can detect weak precipitation that either does not reach the ground or may arrive at locations other than the gauge due to horizontal wind velocity and shear in the boundary layer.

The imposition of threshold values ( $R_0, Z_0$ ) can help alleviate some of the above problems to the extent that they can impose physically consistent sampling regimes. A threshold consistent with the lowest rain intensities measurable by both radar and gauges would seem a good starting point.

**Analytic formulation of probability matching**

There are strong indications that rain rates exhibit a log-normal distribution as described by Krajewski and Smith (1991); Kassim and Kottegoda (1991); Kedem et al. (1990,1994); Atlas et al. (1990), and many others.

The log-normal distribution of  $R$  with two parameters of mean ( $m$ ) and standard deviation ( $\sigma$ ) is described as follows:

$$f(R;\sigma,m) = \frac{1}{\sigma R(2\pi)^{0.5}} \exp[-\frac{1}{2}(\frac{\log R-m}{\sigma})^2] \quad \dots 4$$

Similarly the radar reflectivity factor  $Z$  has also been found to fit a log-normal distribution, (e.g. Atlas et al. 1990; Krajewski and Smith 1991).

In order to verify these probability distribution characteristics, a quantile-quantile plot (QQ-plot) is used here for determining whether the Darwin  $Z$  and  $R$  data exhibit a log-normal distribution. A QQ-plot is actually calculated through the probability density matching. For a QQ-plot, if the samples do come from the same distribution, the plot will be linear. Figure 3 shows QQ-plots comparing  $Z$  and  $R$  at each of the 22 gauges; the vertical coordinate gives the quantile of rainfall rate (in Fig. 3(a)) or reflectivity (in Fig. 3(b)), while the horizontal coordinate gives the quantile from a log-normal distribution generated by random numbers with their mean and variances. The QQ-plot corresponding to each gauge has been shifted horizontally in Fig. 3 in order to avoid overlapping. The plots are essentially linear, which suggest the assumption of log-normality is reasonable.

The  $\chi^2$  goodness-of-fit hypothesis test can also provide a probability value to associate with the fit of  $R$  and  $Z$  histograms to log-normal distributions. Here the average  $\chi^2$  values of  $R$  and  $Z$  at all gauge locations were 16.2 and 21.6 (with 13 degrees of freedom). For a typical significance level of five per cent, the critical  $\chi^2$  value is 22.4 (the null hypothesis is that the experimental data come from the log-normal probability distribution). Because the  $\chi^2$  values are less than the critical value, the hypothesis that the experimental data are log-normally distributed seems acceptable.

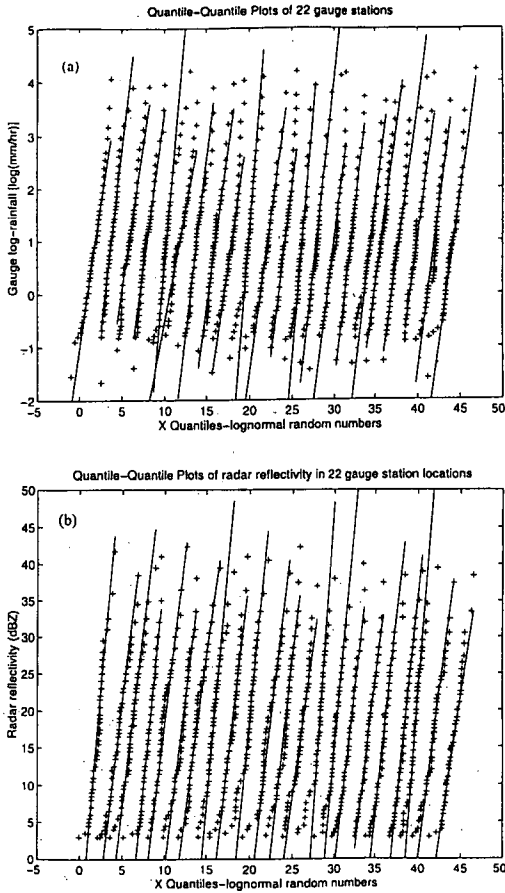
Given that  $Z$  and  $R$  are both log-normally distributed it seems reasonable to formulate probability matching of rainfall rate and reflectivity on this assumption. Integration of Eqn 3 with log-normal distribution functions (Eqn 4) for  $R$  and  $Z$ , yields:

$$\int_0^{Z_i} \frac{1}{\sigma_1 Z(2\pi)^{0.5}} \exp[-\frac{1}{2}(\frac{\log Z-m_1}{\sigma_1})^2] dZ = \int_0^{R_i} \frac{1}{\sigma_2 R(2\pi)^{0.5}} \exp[-\frac{1}{2}(\frac{\log R-m_2}{\sigma_2})^2] dR \quad \dots 5$$

The above equation can be written in differential form as:

$$\exp[-\frac{1}{2}(\frac{\log Z-m_1}{\sigma_1})^2] d(\frac{\log Z}{\sigma_1}) = \exp[-\frac{1}{2}(\frac{\log R-m_2}{\sigma_2})^2] d(\frac{\log R}{\sigma_2}) \quad \dots 6$$

Fig. 3 Quantile-Quantile plots of gauge rainfall (a) and radar reflectivity (b) in 22 gauge stations versus the random numbers generated by log-normal distributions.



by using the first moment estimates of log-normal distributions of rainfall and reflectivity.

If we assume a power law  $Z=AR^\alpha$ , then:

$$\alpha = \frac{\sigma_1}{\sigma_2} \quad \dots 9$$

$$A = e^{(m_1 - \frac{\sigma_1}{\sigma_2} m_2)} \quad \dots 10$$

If Eqn 7 is plotted on a log-log scale, it shows as a straight line, which is equivalent to a rain-gauge-adjusted version of a power law. Clearly, this relationship provides an intrinsic connection between power law and probability matching approaches.

Typically Eqn 6 is not fully suitable for fitting the rainfall and rain-gauge data. Obviously this is a zero threshold approach, in other words, Eqn 4 is for a variable extending from zero to infinity. Systematic errors can result if thresholds are employed because a large proportion of the data is effectively truncated. Hence a conditional probability match should be used, and we fit the data to a modified three-parameter log-normal distribution to incorporate threshold effects normally present in the data analysis. This distribution is of the form:

$$f(R;R_0,\sigma,m) = \frac{1}{\sigma(R-R_0)(2\pi)^{0.5}} \exp[-\frac{1}{2}(\frac{\log(R-R_0)-m}{\sigma})^2] \quad \dots 11$$

Details of this distribution can be found in Crow and Shimizu (1988). In Eqn 11 the rainfall threshold  $R_0$  is included as a distribution parameter. This so-called truncated log-normal distribution ensures that at the thresholds the probability density function tends to zero ( $\log(R-R_0)$  tends to  $-\infty$ ). In the same way,  $Z$  is also fitted to a truncated log-normal distribution.

Fitting this kind of distribution indicates good fits to the rainfall and radar reflectivity probability densities, especially improving the fitting around the left side of the log-normal curve. Similar to Eqn 6, we get:

$$\frac{\log(Z-Z_0)-m_1}{\sigma_1} = \frac{\log(R-R_0)-m_2}{\sigma_2} \quad \dots 12$$

This  $Z$ - $R$  relation is thus determined by three parameters; the mean ( $m$ ), the standard deviation ( $\sigma$ ) and the thresholds. Only the thresholds  $R_0$  and  $Z_0$  are independent parameters, while  $m$  and  $\sigma$  are dependent on the datasets once  $R_0$  and  $Z_0$  are determined. It is obvious that as  $R_0$  and  $Z_0$  tend to zero, Eqn 12 becomes equivalent to Eqn 7.

In order to compare the results calculated by relation 12 with the empirical matching in the previous section, we use the same thresholds,  $R_0>0$ ,  $Z_0=3$  dBZ and  $R_0=1.2$  mm h<sup>-1</sup>,  $Z_0=21$  dBZ respectively (in

It is easily seen that Eqn 6 is valid if and only if it satisfies the following relation:

$$\frac{\log Z - m_1}{\sigma_1} = \frac{\log R - m_2}{\sigma_2} \quad \dots 7$$

or, in the format of dBZ:

$$\frac{dBZ - m'_1}{\sigma'_1} = \frac{\log R - m_2}{\sigma_2} \quad \dots 8$$

Where  $m_1$  is the mean and  $\sigma_1$  is the standard deviation of  $Z$ ;  $m_2$  is the mean and  $\sigma_2$  is the standard deviation of  $R$  (all values are log-scale while  $m'_1$  and  $\sigma'_1$  are in dBZ-scale). Equation 7 can alternatively be derived

Eqn 12 the units of  $Z$  are ( $\text{mm}^6/\text{m}^3$ ). Figures 4 and 5 show the results of employing this analytically based approach for the 22 gauge sites. Compared with Figs 1 and 2, Figs 4 and 5 correctly reproduce the essential characteristics of the empirical  $Z$ - $R$  matches at the two threshold sets. Further calculations at other thresholds consistently show  $Z$ - $R$  relations of Eqn 12 reproduce nearly the same variations as those obtained by using the techniques of the previous section. In other words, Eqn 12 has provided an analytic basis apparently equivalent to the empirical probability matching. In Figs 4 and 5, the matched lines of 22 gauges do not overlap mainly because of the range-dependence.

Equation 12 directly relates the basic population statistical parameters of mean and standard deviation to a  $Z$ - $R$  relationship. Simply calculating the mean and standard deviation of  $Z$  and  $R$  using a set of data, together with the selected thresholds, provides concise and simple  $Z$ - $R$  relations. Because the inherent distributions are known, these statistical parameters reflect the rainfall characteristics as well as the radar-observed storm properties. For the Darwin data used here, the resulting  $Z$ - $R$  relation is near the gauge-radar adjusted power law formula  $Z=75R^{1.25}$ , developed by Steiner et al. (1994), at least with  $Z_0=21$  dBZ and  $R_0=1.2 \text{ mm h}^{-1}$ .

Equation 12 has a simple mathematical expression derived from the log-normal distribution. It is very difficult to derive a  $Z$ - $R$  relationship such as Eqn 12 using other probability distributions.

### Optimisation algorithm for $Z$ - $R$ relations

Whatever the different  $Z$ - $R$  relationships used, there are usually errors present in the radar rainfall measurements. The errors include the effects of :

- (a) measurement errors, as discussed by many authors (e.g. Krajewski and Smith, 1991);
- (b) approximations of the physical processes within the relations;
- (c) differing spatial and temporal scale resolutions of the radar and gauges.

In multivariate statistical analysis, these kinds of errors can be regarded as a model error. Smith and Krajewski (1993) and Krajewski and Smith (1991) presented the error process of a statistical power law of the form:

$$R(t) = \alpha Z(t)^\beta \epsilon(t) \quad \dots 13$$

where  $\epsilon$  is a multiplicative error term.  $R$  is replaced by using raingauge rainfall. By choosing the parameters

**Fig. 4** Probability matching results of rainfall and radar reflectivity using Eqn 12 with thresholds of  $Z_0=3$  dBZ;  $R_0>0$  mm/h.

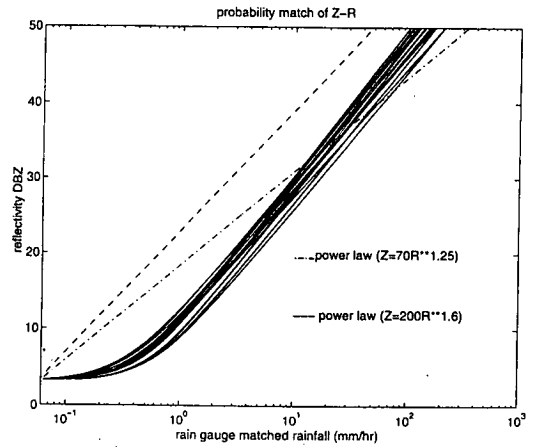
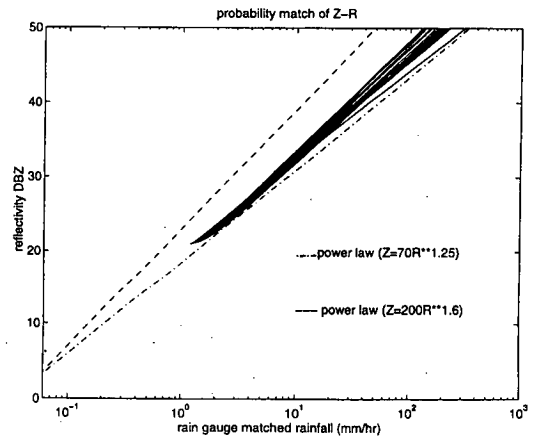


**Fig. 5** Probability matching results of rainfall and radar reflectivity using Eqn 12 with thresholds of  $Z_0=21$  dBZ;  $R_0=1.2$  mm/h.



$\alpha$  and  $\beta$ , it is possible using Eqn 13 to make the model error  $\epsilon$  a minimum. In our application, the objective is to optimally select parameters such as  $R_0$  and  $Z_0$  values which minimise the model errors.

Rather than directly calculating error  $\epsilon$  in Eqn 13, an object function (OF) can be defined by a least square error model as:

$$OF = \min \sum_{i=1}^n [R_{\text{radar}, i}(R_0, Z_0) - R_{\text{gauge}, i}]^2 \quad \dots 14$$

Here, the OF is calculated using the observed 10-minute time series of gauge  $R_{\text{gauge},i}$  subtracted from the radar  $R_{\text{radar},i}$ , calculated by Eqn 12 employing thresholds of  $R_0$  and  $Z_0$ . The summation index  $n$  in Eqn 14 is the number of time intervals. The above OF calculation gives rainfall errors between the observed and radar estimated rainfall rates at individual gauge stations. It is obvious the errors depend heavily on the parameters chosen, therefore the OF is determined by the best parameter set  $R_0$  and  $Z_0$  which optimises the model random errors.

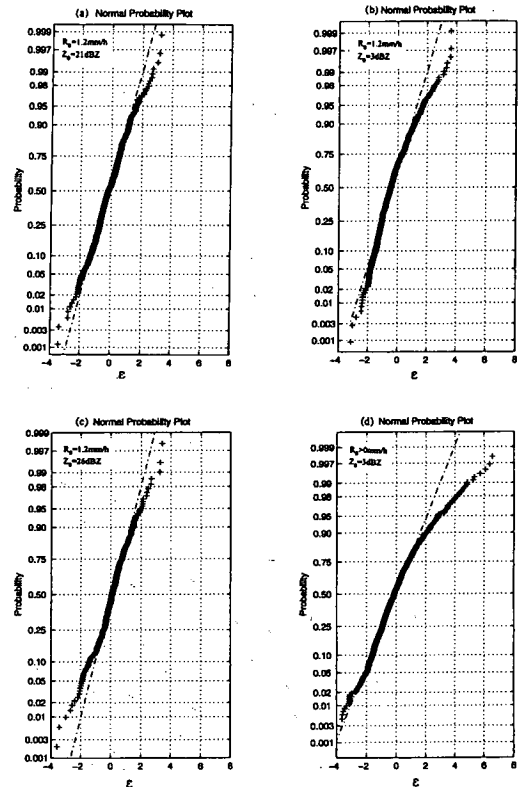
It is difficult to estimate the parameters by direct calculation of the OF. This is a nonlinear case and the use of global searches is ineffective. Secondly, the sample values, and number of samples, of different  $R_0$  and  $Z_0$  can vary and make the values in Eqn 14 incomparable. For example, it may bias the OF values if the OF is just divided by the number of gauge samples.

Kuczera (1990), Kuczera and Williams (1992) and Box and Tiao (1973) provided a method to estimate the nonlinear parameters. This statistical theory states that, if the error  $\epsilon$  is independently and normally distributed with zero mean and constant variance, then there is an optimised parameter vector  $\theta$  which minimises the OF. We follow this approach.

First, the condition of constant error variance was tested by calculating the predicted rainfall to make sure that greater than 95 per cent of the error values were within the variance values. Then the error probability distributions were analysed by plotting the normal distributions of errors. Figure 6 is an example at one gauge station of normal probability plots of error distributions  $\epsilon$  on a logarithmic error scale. From the figure, we can visualise the parameter structure. Here, four different sets of initial parameters are chosen; the first three plots (Figs 6(a), (b) and (c)) are for fixed rainfall thresholds ( $R_0=1.2 \text{ mm h}^{-1}$ ) with different reflectivity thresholds ( $Z_0=21$ ; 3; and 26 dBZ), the last one (Fig. 6(d)) is for  $R_0>0 \text{ mm h}^{-1}$ ,  $Z_0=3 \text{ dBZ}$ . Obviously the condition of  $R_0=1.2 \text{ mm h}^{-1}$ ,  $Z_0=21 \text{ dBZ}$  (Fig. 6(a)) gives the best normalised probability distribution compared to the others, i.e., an error expectation equal to zero (mean equals 0.003 in Fig. 6(a)), and has the least deviation from the straight lines. This condition is consistent with a minimum in the OF. The other thresholds more or less bias the normal distribution with non zero error expectations. In Figs 6(b) and 6(c) the mean errors are -0.31 and 0.15 respectively.

In summary, the diagnostic normal probability plots indicate that the errors are influenced by the parameter vector. Correctly choosing parameters will ensure an optimal solution.

**Fig. 6** Plots of error normal probability distribution with different reflectivity and rainfall thresholds. (a) Thresholds:  $R_0=1.2 \text{ mm/h}$ ;  $Z_0=21 \text{ dBZ}$ . (b) Thresholds:  $R_0=1.2 \text{ mm/h}$ ;  $Z_0=3 \text{ dBZ}$ . (c) Thresholds:  $R_0=1.2 \text{ mm/h}$ ;  $Z_0=26 \text{ dBZ}$ . (d) Thresholds:  $R_0>0 \text{ mm/h}$ ;  $Z_0=3 \text{ dBZ}$ .



## Conclusion

In this paper, using the Darwin radar and rain-gauge network data, we have proposed an alternative methodology to determine radar reflectivity-rainfall relationships. The probability matching or Z-R transformation is derived based on the assumption that Z and R are both log-normally distributed. The calculation of respective population mean and standard deviations, coupled with the assumed nature of the distribution, enables a complete statistical representation of the climatic characteristics of the sample to be obtained. Then, with an analytic form of the respective distributions, direct calculation of PMM relationships is possible. The approach is easy and correctly

reflects the empirically based probability matching results. Depending on threshold selection, the results are also consistent with power law results. We would like to emphasise that in no way do we claim a complete description of the true distribution of rainfall and reflectivity. However, a three parameter log-normal distribution with thresholds is considered to produce acceptable approximations of the empirically derived  $Z$  and  $R$  distributions.

The optimisation methodology used here demonstrates that threshold selection is important in the calculation of  $Z$ - $R$  relationships. This kind of error analysis can also be used to determine the errors inherent in power law rainfall parameters and other rainfall error analyses. Equation 12 derived here has great operational potential, and is easy to implement. Because of the importance of the spatial distribution of rainfall, further research is needed, for example, in combining the spatial statistical analysis (e.g. kriging and cokriging) to improve the prediction of spatial rainfall distribution in a whole radar observation domain.

## Acknowledgments

The authors would like to thank Jim Elliott of the Bureau of Meteorology Hydrology Branch for his assistance and suggestions. This work is part of a flood forecasting project (Project D4) of the Cooperative Research Centre of Catchment Hydrology, Australia.

## References

- Atlas, D., Rosenfeld, D., Amitai, E. and Wolff, D.B. 1990. Classification of rain regimes by the three-dimensional properties of reflectivity fields. *Jnl appl. Met.*, 29, 1120-35.
- Battan, L.J. 1973. *Radar Observations of the Atmosphere*. The University of Chicago Press, Chicago, 324pp.
- Box, G.E.P. and Tiao, G.C. 1973. *Bayesian inference in statistical analysis*. Addison-Wesley, Reading, MA, 588pp.
- Calheiros, R.V. and Zawadzki, I. 1987. Reflectivity-rain rate relationships for radar hydrology in Brazil. *Jnl Clim. appl. Met.*, 26, 118-32.
- Crow, E.L. and Shimizu, K. 1988. *Lognormal distributions*. Marcel Dekker, New York, 387pp.
- Kassim, A.H.M. and Kottegoda, N.T. 1991. Rainfall network design through comparative kriging methods. *Hydrological Science-Journal*, 36, 3, 223-40.
- Kedem, B.H., Chiu, L.S. and North, G.R. 1990. Estimation of real rain rate: Application to satellite observations. *J. geophys. Res.*, 95(D2), 1965-72.
- Kedem, B., Pavlopoulos, H., Guan, X. and Short, D. 1994. A probability distribution model for rain rate. *Jnl appl. Met.*, 33, 1486-93.
- Keenan, T.D. and Carbone, R.E. 1992. A preliminary morphology of precipitation systems in tropical northern Australia. *Q. Jl R. Met. Soc.* 118, 283-326.
- Keenan, T.D., Holland, G.J. and Manton, M.J. 1988. TRMM ground truth in a monsoon environment: Darwin, Australia. *Aust. Met. Mag.*, 36, 81-90.
- Krajewski, W.F. and Smith, J.A. 1991. On the estimation of climatological  $Z$ - $R$  relationships. *Jnl appl. Met.*, 30, 1436-45.
- Kuczera, G. 1990. Assessing hydrologic model nonlinearity using response surface plots. *Jnl Hydrol.*, 118, 143-61.
- Kuczera, G. and Williams, B.J. 1992. Effect of rainfall errors on accuracy of design flood, *Water Resources Research*, 28, 1145-53.
- Rosenfeld D., Wolff, D.B. and Atlas, D. 1993. General probability-matched relations of radar reflectivity and rain rate. *Jnl appl. Met.*, 32, 50-72.
- Rosenfeld D., Amitai, E. and Wolff, D.B. 1995a. Classification of rain regimes by the 3-dimensional properties of reflectivity fields. *Jnl appl. Met.*, 34, 198-211.
- Rosenfeld D., Amitai, E. and Wolff, D.B. 1995b. Improved accuracy of radar WPMM estimated rainfall upon application of objective classification criteria. *Jnl appl. Met.*, 34, 212-23.
- Smith, J.A. and Krajewski, W.F. 1993. A modelling study of rainfall rate-reflectivity relationships. *Water Resources Research*, 29, 2505-14.
- Steiner, M., Houze, R.A., Yuter, S.E., Tenerelli, J. and Brodzik, S.R. 1994. Description of University of Washington algorithms. Preprints, *TRMM Ground Validation Algorithm Intercomparison Workshop*, Seattle, Washington, 1-4.